10.1098/rsta.2003.1211

THE ROYAL SOCIETY

Quantum information with neutral atoms as qubits

By J. V. Porto, S. Rolston, B. Laburthe Tolra, C. J. Williams and W. D. Phillips

National Institute of Standards and Technology, 100 Bureau Drive, Gaithersburg, MD 20899-8424, USA

Published online 30 May 2003

One of the essential features of a quantum computer is a quantum 'register' of well-characterized qubits. Neutral atoms in optical lattices are a natural candidate for such a register. We have demonstrated a patterned-loading technique that can be used to load atoms into large arrays of tightly confined but optically resolvable lattice sites. We have also seen preliminary indications of the Mott-insulator transition, which provides a route for single-atom initialization of the individual sites. Combining the two experiments should allow for large arrays of individually addressable single atoms, a system which provides a starting point for further quantum computation studies.

Keywords: optical lattice; Bose–Einstein condensates; quantum information

1. Introduction

The traditional requirements for a scalable quantum processor are the ability to create large numbers of qubits in well-characterized states, to efficiently and coherently control the individual qubit states, to control qubit interactions, and to accurately measure the system, all while avoiding environment-induced decoherence (DiVincenzo 2000). Trapped neutral atoms provide an attractive system in which to explore experimental quantum information processing (Brennen *et al*. 1999, 2000; Briegel *et al*. 2000), since neutral atoms (including those in far-off resonance optical traps) are inherently weakly coupled to the environment and years of research in atomic/optical physics have produced a range of techniques for the coherent control and measurement of atomic states. Moreover, all atoms of a given isotopic species are identical, in contrast with manufactured qubits, which may be similar but not quantum mechanically identical. The internal hyperfine states of alkali atoms are particularly well suited for making qubits (although there are also proposals for using the external motional states (Charron *et al*. 2002)). Our research programme is aimed at satisfying these requirements using neutral ^{87}Rb atoms, specifically by demonstrating accurate single-atom measurement and control, large-scale state initialization, and producing the controlled interactions needed to perform two-particle gates.

One contribution of 20 to a Discussion Meeting 'Practical realizations of quantum information processing'.

To address the above issues with neutral atoms, most of the proposed schemes require control of both the centre-of-mass and internal states of the atoms, a fact which has motivated research into single-atom magnetic (see, for example, Folman *et al*. 2000; Reichel *et al*. 2001) or optical (see, for example, Dumke *et al*. 2002; Schlosser *et al*. 2001; Frese *et al*. 2000) traps. Using well-understood induced-dipole optical forces, we can create arrays of traps from optical standing waves (Jessen & Deutsch 1996). These optical lattices are easily produced by intersecting laser beams, and can provide tight confinement in large, defect-free arrays of sites in one, two and three dimensions. The lattice position, site spacing and trap depth can be controlled by varying the relative phase, angle and intensity, respectively, of the incident light beams. These properties make the optical lattice a promising candidate for a neutral-atom quantum 'register'.

In the work presented here, we address the following question: given an array of traps provided by an optical lattice, how can we place a large number of individually addressable atoms into the ground state of the lattice sites? The approach we take is to load atoms from a Bose–Einstein condensate (BEC) directly into an optical lattice. Experiments in our laboratory have previously shown (Denschlag *et al*. 2002) that by adiabatically turning on lattice light, a BEC can be loaded with high fidelity into the lowest band of an optical lattice. Time-dependent interferences (beating) arising from non-adiabatic loading provide a sensitive measure of the degree of non-adiabaticity, and we measured a ground band loading efficiency of at least 99.6%. A growing number of experiments (see, for example, Cristiani *et al*. 2002; Pedri *et al*. 2001; Greiner *et al*. 2001) have been performed on BECs loaded into optical lattices. An important challenge for quantum information is to provide individual addressability while maintaining *single* atom initialization of lattice sites. We report here on progress toward that goal.

2. Experiment

The source of atoms in our experiment is a BEC of ^{87}Rb atoms magnetostatically trapped in either the $|F, m_F\rangle = |2, 2\rangle$ or $|1, -1\rangle$ hyperfine ground state, produced using standard laser cooling and evaporative cooling techniques (Cornell & Wieman 2002; Ketterle 2002). The cigar-shaped BEC has approximately a 3:1 aspect ratio resulting from trap frequencies of $\nu_z = 12$ Hz (9 Hz) and $\nu_\rho = 36$ Hz (26 Hz) for the $|F, m_F\rangle = |2, 2\rangle$ ($|1, -1\rangle$) atoms. These magnetically trappable states are obvious ones to load into an optical lattice; however, any two of the eight available ground-state hyperfine levels could be used as the qubit states. The actual choice depends both on the nature of the trap and on which two-qubit gate is implemented.

The lattice potential is provided by the dipole force (Cohen-Tannoudji *et al*. 1992), which scales as I/δ, where I is the laser intensity and δ is the frequency detuning from atomic resonance. Since the spontaneous scattering rate scales as I/δ^2, this possible source of decoherence can be made negligible by increasing the detuning while maintaining the potential depth by also increasing the intensity. Our lattices are produced by intersecting two or more beams from a Ti : sapphire laser at the position of the BEC (see figure 1). (The magnetic trap was kept on during all the lattice experiments described here.) The resulting lattice spacing, d, is determined by the wavelength, λ, of the laser light and the angle, θ, between the beams: $d = \lambda/(2 \sin \theta/2)$. In general, the interference pattern from $D + 1$ independent beams creates a stable

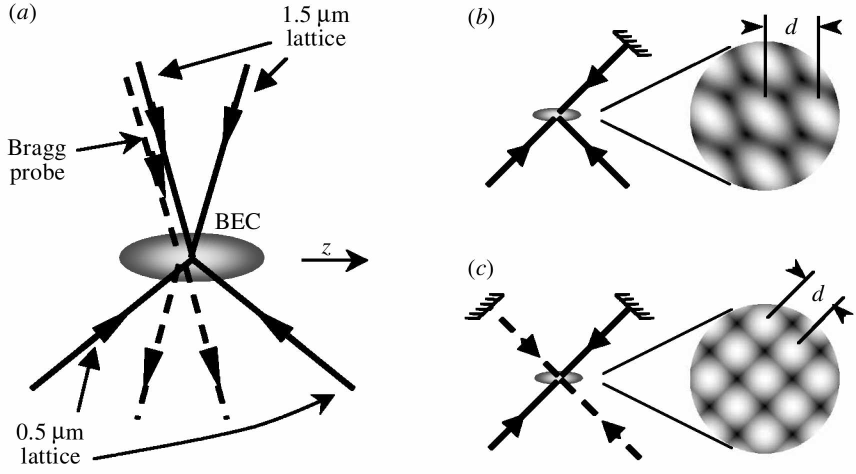

Figure 1. Schematic of typical experimental arrangements. (*a*) Two independent one-dimensional (1D) lattices (spacings of 0.5 μm and 1.5 μm) are aligned along the z-direction. Reflection of a near-resonant Bragg beam incident along one of the lattice beams probes the atomic density distribution at 1.5 μm spacing. (*b*) A two-dimensional (2D) lattice comprising three coplanar equal frequency beams, and a grey-scale plot of the resulting potential. The whitest areas represent the potential minima, which have a minimum lattice spacing of $\sqrt{2}(\lambda/2) \simeq 0.5$ μm. (*c*) A 2D lattice comprising two counter-propagating pairs of detuned beams, resulting in a square lattice potential with $\lambda/2 \simeq 0.39$ μm spacing.

D-dimensional lattice (Grynberg *et al.* 1993). Alternatively, different independent (non-interfering) lattices can be produced by combining separate sets of interfering beams which are detuned from other sets. A 2D lattice can be created, for example, from three beams of equal frequency or from two pairs of beams with different frequencies, each pair separately making a 1D lattice (see figure 1*b*, *c*).

We use two different techniques to characterize the lattice and atomic states. Atom diffraction (see, for example, Ovchinnikov *et al.* 1999) is a convenient tool for characterizing the lattice when the atomic wave function has a well-defined phase throughout the sample. The spatial periodicity of the wave function at period d gives rise to discrete momentum components spaced by h/d, which can be directly measured in free expansion time of flight (see, for example, figure 2*a*, *b*). The number and relative amplitude of diffraction spots provides a measure of the confinement, since the size of the wave function at each site determines the total spread in the momentum distribution. Optical Bragg reflection (Birkl *et al.* 1995), on the other hand, is useful even when there is not a well-defined phase of the atomic wave function across lattice sites. By reflecting a probe beam from the periodic array of atoms, we obtain a phase insensitive measure of the atomic density at the spatial frequency satisfying the Bragg condition.

(*a*) *Patterned loading of an optical lattice*

Atoms can be addressed for optical measurement/control by imaging individual atom sites or focusing a laser beam on an individual site, as has been demonstrated for trapped ions (Raizen *et al.* 1992) and atoms (Scheunemann *et al.* 2000). In order to individually address atoms in a trap array, the atomic spacing needs to be above

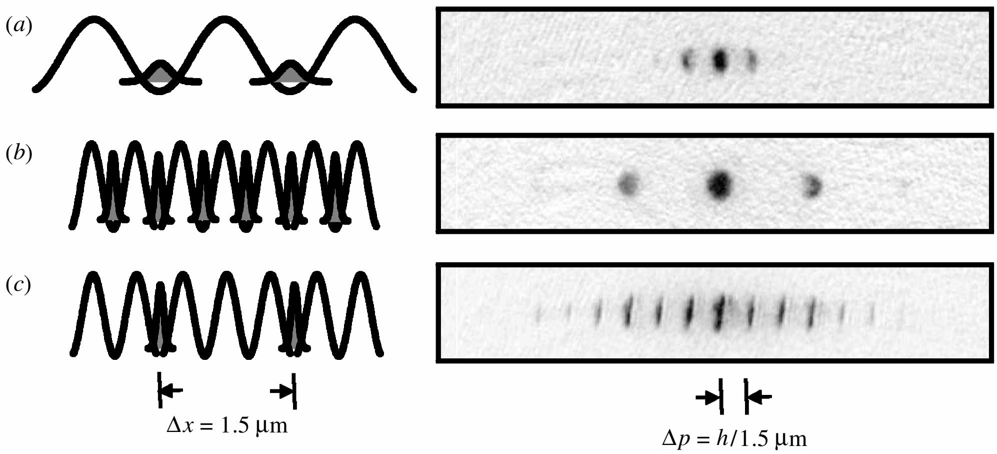

Figure 2. Absorption images showing atom-diffraction patterns from atoms (a) in a $2E_R$ deep, 1.5 μm lattice, (b) in a $20E_R$ deep, 0.5 μm lattice, (c) patterned loaded into every third site of the same 0.5 μm lattice. In each case, the spatial periodicity of the wave function at Δx (shown schematically in the left-hand column) gives rise to discrete momentum components spaced at $h/\Delta x$. The patterned loaded state has momentum components indicative of the 1.5 μm lattice. The lattice light was detuned *ca.* 100 GHz below the D2 line of ^{87}Rb, and the image was taken after 22 ms of free expansion. (The narrowing of the diffraction peaks is the result of a lensing effect due to the non-uniform intensity distribution of the lattice beams along the lattice, resulting in a quadratic phase variation of the wave function. This causes the BEC to 'focus' during the time of free expansion.)

the diffraction limit of the imaging system used to control or measure the atom. At the same time, many time-scales for gate operation and atom movement in the optical lattice 'register' are set by the degree of confinement: tighter confinement allows for faster gates and atom movement. Tighter confinement also allows the atoms to be in the Lamb–Dicke limit, and therefore less susceptible to motional decoherence by spontaneous emission. In an optical lattice, these two requirements are at odds: a longer period lattice provides wide spacing, but also weaker confinement. We demonstrate here that by using two independent lattices with different periods to form a 'superlattice', we can simultaneously satisfy both criteria, with atom spacing determined by one lattice and atom confinement by the other.

Atoms can be loaded into every nth site of a lattice by the sequential application of two independent lattices whose periods differ by a factor of n (Peil *et al.* 2003). To demonstrate the technique, we used two 1D lattices with periods of $d_1 = 1.5\,\mu\text{m}$ and $d_2 = 0.5\,\mu\text{m}$, such that $n = d_1/d_2 = 3$ (see figure 1a). (The 1.5 μm spacing we chose is below the resolution of our current imaging optics, but improved optics or extending the technique to higher n can make the trapped sites resolvable.) First, the 1.5 μm lattice is turned on to localize the atoms at its lattice sites. The 0.5 μm lattice is then turned on, localizing the atoms at those of its lattice sites that are closest to the 1.5 μm sites. Turning off the long-period lattice leaves the atoms well localized in every third site of the short lattice. Atom diffraction from the patterned loaded state is shown in figure 2c. To obtain these pictures, the loading sequence was performed slowly enough that no excitation of atomic vibrational motion in the individual potential wells of the optical lattice (i.e. no band excitation) occurred. The loading

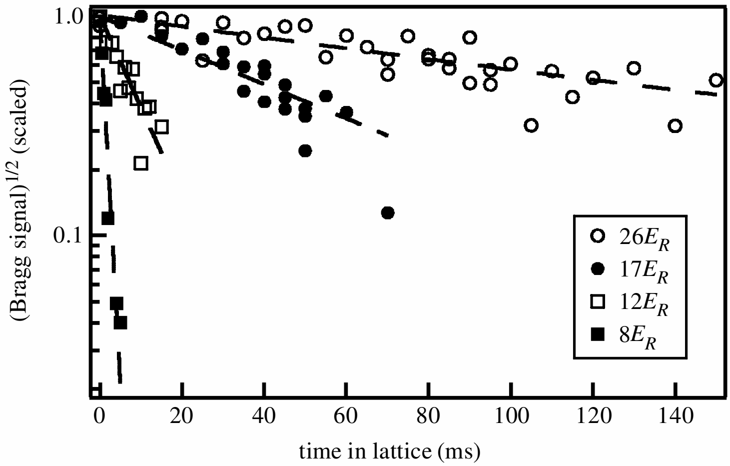

Figure 3. Direct observation of atom tunnelling in a 3D lattice. At $t = 0$ atoms are patterned loaded into every third plane of a 3D lattice. (The lattice beams were detuned below the D2 line of ^{87}Rb by 1 nm.) The 'every third' population is monitored (using Bragg reflection of a probe beam) as a function of time for different lattice depths. The lattice depth indicated is the peak-to-peak depth of the periodic potential *along the direction of tunnelling*. The straight lines are exponential fits to the data, giving time constants of 1.3 ms, 10 ms, 55 ms and 150 ms.

is, however, quick enough to avoid interaction-induced number squeezing (Greiner *et al.* 2002; Orzel *et al.* 2001) and interaction-induced dephasing (Mandel *et al.* 2003), thus preserving the phase coherence necessary for atom diffraction. The atoms diffracted from the patterned loaded state have momentum spacing indicative of the 1.5 µm lattice, even though the long-period lattice has been completely removed (compare figure 2*c* with figure 2*a*, *b*). To confirm that atoms are indeed loaded only into every third site, we used a phase-insensitive probe: optical Bragg diffraction of a near-resonant probe beam from the atom distribution. The probe beam was incident at the first-order Bragg condition for the 1.5 µm lattice (see figure 1*a*). Since this corresponds to a fractional order for the 0.5 µm lattice, we expect no diffraction from atoms loaded into every site. We observe *ca.* 100% reflectivity from patterned loaded atoms, and detect no reflection from atoms loaded into every site of the 0.5 µm lattice.

The patterned-loading technique can easily be extended to two and three dimensions. For example, we loaded every third plane of a 3D lattice. This is accomplished by first loading a 1D lattice with period $d = 1.5$ µm. Subsequently, an independent shorter-period three-beam 2D lattice ($d = 0.5$ µm, as shown in figure 1*b*) is applied such that one of its axes is aligned with the 1.5 µm 1D lattice, loading atoms into every third row of sites in the 2D lattice. Finally, the original 1D lattice is removed, and applying another independent 1D lattice with a component perpendicular to the 2D lattice produces a patterned loaded 3D lattice, where every third plane of sites is occupied. As discussed above, each of the separate lattices were detuned from each other to ensure that the lattices did not interfere with each other. The patterned structure was confirmed using optical Bragg reflection at the 1.5 µm Bragg condition, which is sensitive only to density distributions matching that wavelength. Using this tool we are able to directly observe tunnelling of atoms from the filled sites to empty sites in a 3D lattice as a function of total lattice depth. In figure 3 we show, as a function of time, the exponential decrease in the Bragg-reflected signal from the patterned loaded lattice for four different lattice depths. The lattice depths are expressed in units of the recoil energy, $E_{\mathrm{R}} = h/2m\lambda^2$. Reducing the lattice depth by a factor of about three results in a decay rate of the patterned loaded state about 100 times larger.

(*b*) *Interaction-induced number squeezing*

While we have demonstrated 'initialization' of the centre-of-mass and internal states of the atom into the ground state of lattice sites, the above experiments did not have a definite number of atoms (e.g. one) per lattice site. The task of initializing single atoms to individual sites can be attempted by laser cooling directly into the lattice (see, for example, Hamann *et al*. 1998; DePue *et al*. 1999; Schlosser *et al*. 2001) and relying on two-body loss mechanisms to remove multiply occupied sites, but it has been proposed (Jaksch *et al*. 1998) and more recently demonstrated that, for sufficiently slow loading from a BEC, repulsive atom–atom interactions lead to number squeezing (Orzel *et al*. 2001) and the Mott-insulator transition (Greiner *et al*. 2002), which can result in single-atom occupation of individual lattice sites in a 3D lattice. The number squeezing results from a competition between tunnelling, which tends to delocalize atoms over many sites, and the interaction energy, which tends to minimize the number fluctuations at a given site. Since delocalized states are characterized by uncertain numbers of atoms per site but a well-defined phase, these states give rise to clear atom diffraction when the lattice is suddenly turned off. The fully number-squeezed state, on the other hand, has well-defined site occupation and uncertain phase, and does not give rise to atom diffraction peaks. As the lattice is turned on, the relative importance of the interaction and kinetic (i.e. tunnelling) energies changes, allowing the delocalized BEC to be adiabatically converted to a state where sites have a definite number of atoms. This conversion is associated with the Mott-insulator transition.

One of the signatures of the Mott-insulator transition is the disappearance of atom diffraction peaks as the lattice depth is slowly (adiabatically) increased, followed by the recovery of diffraction peaks as the lattice is subsequently adiabatically decreased. We have made preliminary observations of such a loss and recovery of phase coherence, as shown in figure 4. In this experiment, the depth of a 3D lattice is smoothly turned on and off over a period of 200 ms. The depth of the lattice is approximately Gaussian in time, except that the lattice and magnetic trap were suddenly turned off at various points during this time to observe the atom diffraction. In these preliminary data, the maximum depth of the lattice was not carefully calibrated, but the diffraction pattern disappears at a lattice depth on the order of $5E_{\mathrm{R}}$–$10E_{\mathrm{R}}$, somewhat below the depth of approximately $13E_{\mathrm{R}}$ expected for a perfect cubic lattice. In our case, the lattice was not cubic and the lattice depths in all three directions were not identical. The disappearance and recovery is evidence for the transition, but additional signatures of the Mott-insulator state (significantly reduced number fluctuations, a gap in the energy spectrum, and a discontinuous change in the transport response to an applied force) remain to be observed. We plan to develop spectroscopic and transport techniques to further study and characterize this system.

Our observations suggest a sensitivity of the recovery of coherence to the stability of the experiment. While the distinct pattern appearing before the loss of diffraction

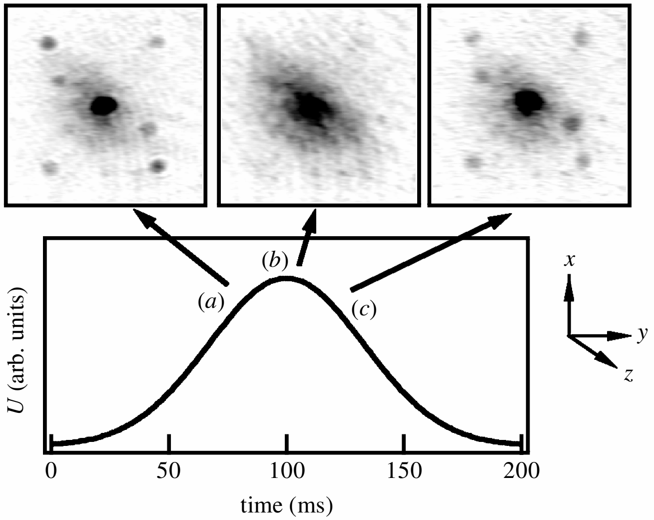

Figure 4. Atom diffraction images observed by turning off the lattice at different points during the application and removal of a 3D optical lattice. For these images the lattice was turned on and removed in 200 ms with an approximately Gaussian shape. The image in (*a*) was obtained while the lattice was being increased toward the peak depth. The image in (*b*) was obtained by switching off the lattice at the peak lattice depth, and the image in (*c*) was obtained after the peak had been reached and subsequently decreased to the same value as in (*a*).

(at point (*a*)) is always observed, the recovery of diffraction at point (*c*) appears to be very sensitive to lattice alignment and residual random BEC motion. The distinct diffraction shown in figure 4*c* was only obtained 75% of the time (otherwise it looked like figure 4*b*). The failure to observe the recovered atom diffraction appears to correlate with random residual motion of the BEC. Once the source of this residual motion can be identified and controlled, we plan to study quantitatively the effect of the BEC initial velocity on the transition.

(*c*) *Combining patterned loading and the Mott state using an 'accordion' lattice*

To get initialized, addressable single atoms, the above techniques for patterned loading and number squeezing need to be combined. One possibility involves driving the Mott transition first, then patterned loading the resulting number-squeezed states. Since the Mott-insulator transition relies on large atom–atom interaction, it is favourable to have tight confinement while driving the transition. The patterned-loading procedure, on the other hand, requires starting with a long-period lattice. To satisfy both criteria, we are developing a variable spacing 'accordion' lattice, where the lattice spacing can be modified by dynamically changing the angle between a pair of lattice beams that are imaged onto the BEC. With the accordion lattice, the Mott state can be first obtained in a short-period lattice and the lattice can be stretched to a larger period for the patterned-loading procedure. A schematic of the accordion design is shown in figure 5. The ability to easily control atom–atom spacing could be useful for a variety of experiments, for example, measurement of light-induced interactions between atoms as a function of distance.

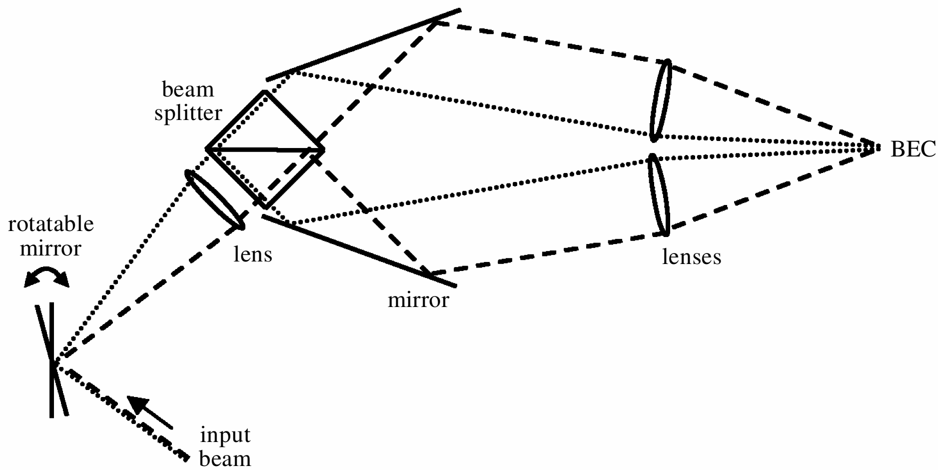

Figure 5. Schematic of the 'accordion' lattice design. The incoming lattice beam is to be reflected from a rotatable mirror, and the point where the beam hits the mirror is imaged onto the BEC via two different paths created with a beam splitter. As the mirror is rotated through an angle θ, the position of the laser-beam intersection does not move, but the angle between the beams changes by 2θ.

3. Outlook

Much of the progress we have made toward neutral-atom quantum computing has focused on addressability and initialization. To show the feasibility of the neutral-atom approach, future experiments must combine addressability and initialization with individual qubit readout and implementation of one- and two-qubit gates on specified qubits. All of this must be accomplished while meeting the stringent limitations on decoherence.

State-specific readout of ions has been demonstrated (Monroe *et al.* 1995) using photon detection from a cycling transition, and a similar approach has recently been used for neutral atoms (e.g. Frese *et al.* 2000; Schlosser *et al.* 2001). Current neutral-atom traps are relatively shallow compared with ion traps, making recoil heating during measurement an important consideration. Increased efficiency readout may be possible using more sophisticated readout schemes that include simultaneous cooling and/or ionization and detection, and we plan to explore such possibilities. Unlike gate fidelity and decoherence requirements, however, high readout efficiency is not strictly required (at least for the final readout of a calculation) because the collection of statistics on repeated measurements only incurs a linear overhead on the quantum calculation.

Single-qubit gates are demonstrated routinely in atomic-clock experiments, and recent experiments by the Munich group (Mandel *et al.* 2003) have demonstrated the controlled interactions needed for building a two-qubit gate. In neither of these cases are gates performed on a select single or pair of qubits. Using patterned loading and two photon Raman techniques, it should be straightforward to perform single-qubit operations on select qubits. An extension of the Raman technique along with an implementation of the Rydberg gate (Jaksch *et al.* 2000) provides one obvious solution to performing a two-qubit gate on a select pair of atoms in an optical lattice. Numerous other approaches for two-qubit gates exist if alternative trapping technologies are employed.

While the largest acceptable decoherence rate for scalable quantum computation remains theoretically unknown, it appears that one requires decoherence times that are 10^3 or 10^4 times longer than typical gate operation times. Unacceptable decoherence can be introduced via coupling to the environment and/or trap, which degrades the quantum 'memory' during and between computations. In addition, noise can be introduced from the control lasers during gates. In principle, the low coupling to the environment for atomic systems provides near ideal memory qubits, as evidenced by their use in high-precision clocks. Heating in dipole traps from amplitude and position noise of the trapping laser is well understood (Savard *et al*. 1997), and measurements and calculations for our system indicate this source of decoherence will not be a problem. The ultimate limitations will most likely result from the implementation of one- and two-qubit gates, the details of which depend on the type of gates used. A full understanding of the limitations requires further experimental and theoretical research, and we plan to study two possible two-qubit gates: the state-selective collisional gate proposed by Jaksch *et al*. (1999) and the Rydberg-blockade gate proposed by Jaksch *et al*. (2000).

4. Conclusions

We have demonstrated the ability to pattern load atoms from a BEC into an optical lattice and seen indications that we can initialize fixed numbers of atoms per lattice site via the Mott-insulator transition. Combining these two techniques should allow us to initialize individual atoms into addressable, tightly confined sites in an optical lattice, providing an interesting system for studying individual one- and two-qubit gates.

This work was supported in part by the Advanced Research and Development Activity/National Security Agency.

References

Birkl, G., Gatzke, M., Deutsch, I. H., Rolston, S. L. & Phillips, W. D. 1995 Bragg scattering from atoms in optical lattices. *Phys. Rev. Lett.* **75**, 2823–2826.

Brennen, G. K., Deutsch, I. H. & Jessen, P. S. 1999 Quantum logic gates in optical lattices. *Phys. Rev. Lett.* **82**, 1060–1063.

Brennen, G. K., Deutsch, I. H. & Jessen, P. S. 2000 Entangling dipole–dipole interactions for quantum logic with neutral atoms. *Phys. Rev.* A **61**, 062309.

Briegel, H. J., Calarco, T., Jaksch, D., Cirac, J. I. & Zoller, P. 2000 Quantum computing with neutral atoms. *J. Mod. Opt.* **47**, 415–451.

Charron, E., Tiesinga, E., Mies, F. & Williams, C. 2002 Optimizing a phase gate using quantum interference. *Phys. Rev. Lett.* **88**, 077901.

Cohen-Tannoudji, C., Dupont-Roc, J. & Grynberg, G. 1992 *Atom–photon interactions*. Wiley.

Cornell, E. A. & Wieman, C. E. 2002 Nobel Lecture: Bose–Einstein condensation in a dilute gas, the first 70 years and some recent experiments. *Rev. Mod. Phys.* **74**, 875–893.

Cristiani, M., Morsch, O., Muller, J. H., Ciampini, D. & Arimondo, E. 2002 Experimental properties of Bose–Einstein condensates in one-dimensional optical lattices: Bloch oscillations, Landau–Zener tunneling, and mean-field effects. *Phys. Rev.* A **65**, 063612.

Denschlag, J. H., Simsarian, J. E., Haffner, H., McKenzie, C., Browaeys, A., Cho, D., Helmerson, K., Rolston, S. L. & Phillips, W. D. 2002 A Bose–Einstein condensate in an optical lattice. *J. Phys.* B **35**, 3095–3110.

DePue, M. T., McCormick, C., Winoto, S. L., Oliver, S. & Weiss, D. S. 1999 Unity occupation of sites in a 3D optical lattice. *Phys. Rev. Lett.* **82**, 2262–2265.

DiVincenzo, D. 2000 The physical implementation of quantum computation. *Fortschr. Phys.* **48**, 771–783.

Dumke, R., Volk, M., Muether, T., Buchkremer, F. B. J., Birkl, G. & Ertmer, W. 2002 Micro-optical realization of arrays of selectively addressable dipole traps: a scalable configuration for quantum computation with atomic qubits. *Phys. Rev. Lett.* **89**, 097903.

Folman, R., Krueger, P., Cassettari, D., Hessmo, B., Maier, T. & Schmiedmayer, J. 2000 Controlling cold atoms using nanofabricated surfaces: atom chips. *Phys. Rev. Lett.* **84**, 4749–4752.

Frese, D., Ueberholz, B., Kuhr, S., Alt, W., Schrader, D., Gomer, V. & Meschede, D. 2000 Single atoms in an optical dipole trap: towards a deterministic source of cold atoms. *Phys. Rev. Lett.* **85**, 3777–3780.

Greiner, M., Bloch, I., Mandel, O., Hansch, T. W. & Esslinger, T. 2001 Exploring phase coherence in a 2D lattice of Bose–Einstein condensates. *Phys. Rev. Lett.* **87**, 160405.

Greiner, M., Mandel, O., Esslinger, T., Hansch, T. W. & Bloch, I. 2002 Quantum phase transition from a superfluid to a Mott insulator in a gas of ultracold atoms. *Nature* **415**, 39–44.

Grynberg, G., Lounis, B., Verkerk, P., Courtois, J. Y. & Salomon, C. 1993 Quantized motion of cold cesium atoms in 2-dimensional and 3-dimensional optical potentials. *Phys. Rev. Lett.* **70**, 2249–2252.

Hamann, S. E., Haycock, D. L., Klose, G., Pax, P. H., Deutsch, I. H. & Jessen, P. S. 1998 Resolved-sideband Raman cooling to the ground state of an optical lattice. *Phys. Rev. Lett.* **80**, 4149–4152.

Jaksch, D., Bruder, C., Cirac, J. I., Gardiner, C. W. & Zoller, P. 1998 Cold bosonic atoms in optical lattices. *Phys. Rev. Lett.* **81**, 3108–3111.

Jaksch, D., Briegel, H. J., Cirac, J. I., Gardiner, C. W. & Zoller, P. 1999 Entanglement of atoms via cold controlled collisions. *Phys. Rev. Lett.* **82**, 1975–1978.

Jaksch, D., Cirac, J. I., Zoller, P., Rolston, S. L., Cote, R. & Lukin, M. D. 2000 Fast quantum gates for neutral atoms. *Phys. Rev. Lett.* **85**, 2208–2211.

Jessen, P. S. & Deutsch, I. H. 1996 Optical lattices. In *Advances in atomic, molecular and optical physics* (ed. B. Bederson & H. Walther), vol. 37, pp. 95–138. Academic.

Ketterle, W. 2002 Nobel lecture: when atoms behave as waves: Bose–Einstein condensation and the atom laser. *Rev. Mod. Phys.* **74**, 1131–1151.

Mandel, O., Greiner, M., Widera, A., Rom, T., Haensch, T. W. & Bloch, I. 2003 Coherent transport of neutral atoms in spin-dependent optical lattice potentials. (Preprint cond-mat/0301169.)

Monroe, C., Meekhof, D. M., King, B. E., Jefferts, S. R., Itano, W. M., Wineland, D. J. & Gould, P. 1995 Resolved-side-band Raman cooling of a bound atom to the 3D zero-point energy. *Phys. Rev. Lett.* **75**, 4011–4014.

Orzel, C., Tuchman, A. K., Fenselau, M. L., Yasuda, M. & Kasevich, M. A. 2001 Squeezed states in a Bose–Einstein condensate. *Science* **291**, 2386–2389.

Ovchinnikov, Y. B., Muller, J. H., Doery, M. R., Vredenbregt, E. J. D., Helmerson, K., Rolston, S. L. & Phillips, W. D. 1999 Diffraction of a released Bose–Einstein condensate by a pulsed standing light wave. *Phys. Rev. Lett.* **83**, 284.

Pedri, P., Pitaevskii, L., Stringari, S., Fort, C., Burger, S., Cataliotti, F. S., Maddaloni, P., Minardi, F. & Inguscio, M. 2001 Expansion of a coherent array of Bose–Einstein condensates. *Phys. Rev. Lett.* **87**, 220401.

Peil, S., Porto, J. V., Laburthe Tolra, B., Obrecht, J. M., King, B. E., Subbotin, M., Rolston, S. L. & Phillips, W. D. 2003 Patterned loading of a Bose–Einstein condensate into an optical lattice. *Phys. Rev.* A. (In the press.)

Raizen, M. G., Gilligan, J. M., Bergquist, J. C., Itano, W. M. & Wineland, D. J. 1992 Ionic-crystals in a linear Paul trap. *Phys. Rev.* A **45**, 6493–6501.

Reichel, J. W., Haensel, W., Hommelhoff, P. & Haensch, T. W. 2001 Applications of integrated magnetic microtraps. *Appl. Phys.* B **72**, 81–89.

Savard, T. A., Ohara, K. M. & Thomas, J. E. 1997 Laser-noise-induced heating in far-off resonance optical traps. *Phys. Rev.* A **56**, R1095–R1098.

Scheunemann, R., Cataliotti, F. S., Hansch, T. W. & Weitz, M. 2000 Resolving and addressing atoms in individual sites of a CO_2-laser optical lattice. *Phys. Rev.* A **62**, 051801.

Schlosser, N., Reymond, G., Protsenko, I. & Grangier, P. 2001 Sub-Poissonian loading of single atoms in a microscopic dipole trap. *Nature* **411**, 1024–1027.